Dorador, L., Barrera, C.E, Rozas, J. and Villalobos, F.A (2021). Analysis of the effect of fines content and loading frequency on the shear modulus and damping ratio of gravels.
Obras y Proyectos **30**, 39-49

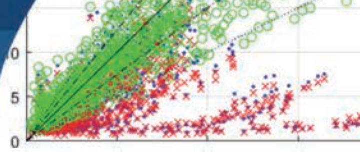

Analysis of the effect of fines content and loading frequency on the shear modulus and damping ratio of gravels

Análisis del efecto del contenido de finos y la frecuencia de carga en el módulo de corte y razón de amortiguamiento en gravas

Fecha de entrega: 20 de agosto 2021
Fecha de aceptación: 10 de noviembre 2021

Leonardo Dorador[1], Carolina E. Barrera[2], Jorge Rozas[3] and Felipe A. Villalobos[3]

[1] EGSciences SpA, Santiago, Chile, info@egsciences.com

[2] Departamento de Obras Civiles, Universidad Técnica Federico Santa María, Vicuña Mackenna 3939, San Joaquín, Chile, carolina.barrera.13@sansano.usm.cl

[3] Departamento de Ingeniería Civil, Universidad Católica de la Santísima Concepción, Alonso de Ribera 2850, Concepción, Chile, jrozas@ing.ucsc.com, avillalobos@ucsc.cl (Orcid: 0000-0002-5419-3958)

The dynamic properties of coarse granular soils have been much less studied than in sands. From a database of 14 gravel samples subjected to cyclic triaxial tests, available relationships are studied and new proposed to estimate the normalised shear modulus G/G_{max} *and the damping ratio D as a function of shear strain* γ*. The effect of confining stress, fines content, uniformity coefficient and loading frequency on the variation of* G/G_{max} *and D versus* γ *is analysed. It is obtained that* G/G_{max} *is dependent on confinement, but not on loading frequency. 85.6% of the data converge in an error band of less than 25% for the proposed formulation. The damping D does depend on fines content as well as confinement and loading frequency. The proposed formulation for D has a 56% probability of having errors less than 25%.*

Keywords: gravels, shear modulus, damping, loading frecuency, fines content

Las propiedades dinámicas de suelos gruesos han sido mucho menos estudiadas que en arenas. A partir de una base de datos de 14 muestras de gravas sometidas a ensayos triaxiales cíclicos, se estudian relaciones disponibles y se proponen nuevas para estimar el módulo de corte normalizado G/G_{max} *y la razón de amortiguamiento D en función de la deformación de corte* γ*. Se analiza el efecto del confinamiento, contenido de finos, coeficiente de uniformidad y frecuencia de carga en la variación de* G/G_{max} *y D versus* γ*. Se obtiene que* G/G_{max} *es dependiente del confinamiento, pero no de la frecuencia de carga. Un 85.6% de los datos converge en una banda de error menor al 25% para la formulación propuesta. El amortiguamiento D sí depende del confinamiento, así como del contenido de finos y de la frecuencia de carga. La formulación propuesta para D posee un 56% de probabilidad de tener errores menores al 25%.*

Palabras clave: gravas, módulo de corte, amortiguamiento, frecuencia de carga, contenido de finos

Introduction

The systematic study of the geomechanical properties of coarse granular materials has historically advanced after that for finer soils such as sands. Special methodologies have had to be developed to analyse coarse granular materials, since laboratory equipment are limited for testing large particles (Ovalle *et al.*, 2020; Dorador and Villalobos, 2020a,b). The study of the dynamic properties of coarse granular material has not been the exception. Since the 1960s several experimental studies have been carried out for the analysis of the dynamic properties of sands to define the shear modulus *G* and damping ratio *D* variation with shear strain γ (*e.g.* Hardin, 1965; Hardin and Drnevich, 1972a,b; Ishihara, 1996; Kramer, 1996; Martínez, 2008; Navarrete, 2009, Wichtmann *et al.*, 2015). However, experimental studies with coarse granular material started later in the middle of the 1980s when larger samples could be tested in cyclic triaxial apparatus as pointed out by Rollins *et al.* (1998), who summarise the early works with gravels.

Soil dynamic response can vary significantly depending on the type of cyclic load to which it is subjected which is, for instance, relevant for the design of dams, foundations, walls, coastal and mining structures. The origin of cyclic loads can be diverse, either produced by seismicity (earthquakes), environment (currents, waves, winds) or anthropic (vibratory machines, traffic, trains). The most important parameters for dynamic analysis are the shear modulus G and the damping ratio D, both parameters depend strongly on the cyclic shear strain γ. At low strain levels (less than 10^{-4}%), common in vibratory machines, these parameters remain essentially constant. However, for higher cyclic loads, the deformation levels can be considerably higher and the variation of G and D as a function of γ should be studied, in order to reduce uncertainty and avoid inappropriate designs.

For gravel samples, Rollins *et al.* (1998) analysed and selected results of available series of tests from 15 research programmes and based on a one parameter hyperbolic formulation, proposed for sands by Hardin and Drnevich (1972a,b), average curves for the evaluation of $G/G_{max} - \gamma$ and $D - \gamma$ were developed. Rollins *et al.* (1998) concluded that $G/G_{max} - \gamma$ and $D - \gamma$ curves were almost independent on sample disturbance, fines content (range 0-9%) and gravel content. Additionally, $G/G_{max} - \gamma$ curves were independent on the relative density. Conversely, $G/G_{max} - \gamma$ and $D - \gamma$ curves were fairly dependent on the confining stress.

Stokoe *et al.* (1999) modify the hyperbolic formulation incorporating a second parameter for adjusting the shape of G-γ curves. Rollins *et al.* (2020) adopting this two-parameter hyperbolic formulation re-assess a database of 18 researchers, confirming the dependence on confining stress σ'_c, and this time also on the grain size distribution in the form of the uniformity coefficient C_u. They confirm the independence on relative density and voids ratio, which has also been found by Menq (2003).

From large scale cyclic triaxial testing of rockfill materials, Araei *et al.* (2012a,b) conclude that the loading frequency f can increase the shear modulus at low strain levels, although this effect reduces as strain increases. The $G/G_{max} - \gamma$ curve decreases with f for a certain value of strain. Damping becomes more affected by f for the whole range of strain level studied. However, these quantitative conclusions were not expressed qualitatively using mathematical relationships.

In this study experimental data available from previous research is analysed in terms of degradation curves of $G/G_{max} - \gamma$ and $D - \gamma$. The effect of confining stress is included in the analyses together with uniformity coefficient and loading frequency. In addition, the effect of fines content is considered, which has been neglected in previous studies. The formulations proposed for the estimation of the dynamic properties for gravels are statistically assessed to quantify their quality and are compared with previous formulations.

Characteristics of the gravels

A data set from 6 different research works with 14 samples was compiled, which comprise cyclic triaxial tests in probes of 300 mm in diameter and 600 and 750 mm in height. The gravel main characteristics, parameters of the laboratory tests and hyperbolic formulations are summarised in Tables 1 and 2, respectively.

From Table 1 it can be noted that the void ratio e varies between 0.161 and 0.329, and the uniformity coefficient C_u between 7 and 272. These low values of e are related to the high values of C_u, which means that non uniform or well graded grain size distributions give place to much higher packing, hence lower voids. The percentage of gravel-size particles ranges between 55 and 86%, while the percentage of fines does between 0.1 and 14% and mean diameter D_{50} between 6 and 19 mm with an average of 11.5 mm, which is above the limit standardized by the Unified Soil Classification System USCS for gravel classification, which corresponds to 4.75 mm or No. 4 sieve (ASTM D2487, 2017). Therefore, the material is predominantly classified as a gravel - well graded sandy gravel GW. Figure 1 shows the particle size distribution of all the samples indicated in Table 1.

Table 1: Characteristics of the gravels analysed in the series of tests

Reference	Sample	Description	Gravel, %	FC, %	D_{50}, mm	C_u	G_s	γ_d, kN/m^3	*e*
Zhou *et al.* (2016)	HZY-1	Limestone rockfills	82.8	1.8	17.34	7.5	--	22.27	0.235
	HZY-2	Limestone rockfills	74.9	2.2	14.20	30.3	--	22.77	0.195
	HZY-3	Limestone rockfills	57.8	5.9	7.85	85.3	--	23.25	0.205
	HZY-4	Rhyolite rockfills	82.8	1.8	17.34	7.5	--	21.58	0.235
	LHK-1	Granite rock grain	85.8	2.4	19.17	8.8	--	20.31	0.241
Araei *et al.* (2012a)	S.G	Modeled shell/ Gotvand	72.6	10.0	15.71	272.1	2.59	21.50	--
	S.3AMES	Dam shell/zone 3A/ MES	55.0	6.5	6.45	68.8	2.64	21.20	0.281
	S.3BMES	Dam shell/zone 3B/ MES	72.0	13.8	10.78	--	2.64	21.80	0.280
Araei *et al.* (2012b)	S.SBU	Lime rock (Upper Siah-Bisheh CFRD)	58.0	3.8	6.50	19.0	2.71	21.50	0.161
Goto *et al.* (1992)	Depth 5 - 6 m	in situ freezing alluvial gravel	52.3	0.1	10.00	37.5	--	20.68	--
	Depth 12 - 13 m		55.0	0.5	6.00	25.0	--	18.91	--
Yasuda and Matsumoto (1994)	Angular	rockfill	84.1	--	14.82	7.0	2.65	--	--
Hatanaka *et al.* (1988)	U-4	in situ freezing	55.0	8.5	5.70	60.0	2.69	19.86	0.329
	U-5	deluvial gravel	65.0	0.8	10.30	13.9	2.69	20.95	0.260

% gravel: > 4.75 mm, FC: fines content, D_{50}: mean grain size, C_u: uniformity coefficient, G_s: specific gravity, γ_d: dry unit weight, *e*: void ratio

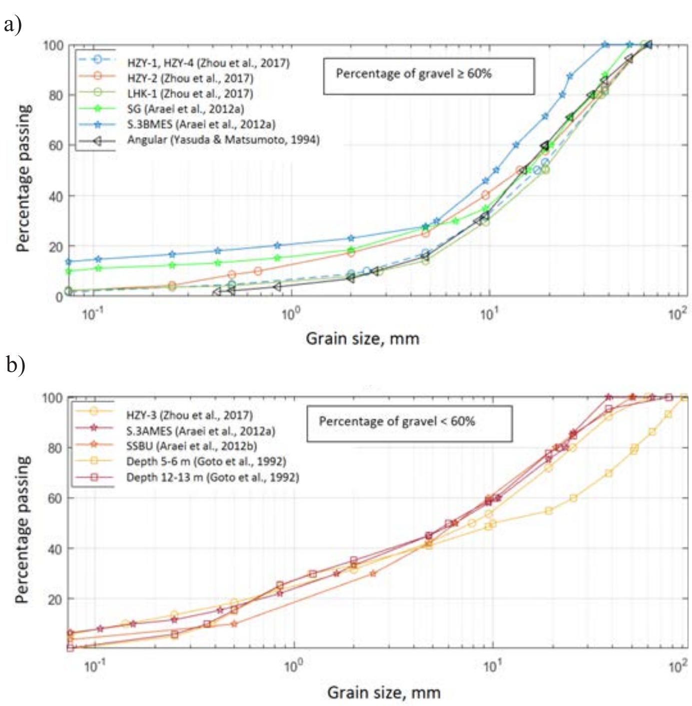

Figure 1: Particle size distribution for: a) more than 60% of gravel and b) less than 60% of gravel

G/G_{max} versus shear strain relation

The representation of the shear modulus *G* with the cyclic shear strain γ, is usually dividing *G* by G_{max}, which is a normalization regularly adopted in practice that allows comparing different results and relationships. Hardin and Drnevich (1972a,b) developed a hyperbolic model widely used in dynamics analysis of sands, which later on was modified by Stokoe *et al.* (1992) incorporating the curvature parameter *m*. This second parameter can improve the fit of experimental data. The two-parameter hyperbolic model can be expressed as:

$$\frac{G}{G_{max}} = \frac{1}{1+\left(\frac{\gamma}{\gamma_{ref}}\right)^m} \quad (1)$$

where the reference deformation γ_{ref} is used to normalize the shear deformation γ such that $G/G_{max} \approx 0.5$ and *m* is a curvature parameter. As *m* increases the shear modulus *G* increases at small shear strains γ and decreases at high levels of γ.

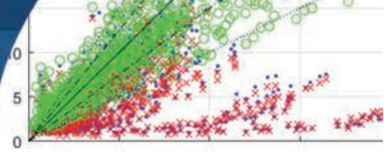

Table 2: Cyclic triaxial test and hyperbolic model parameters

Reference	Sample	d/h, mm/mm	Drainage	No. of cycles	Loading frequency, Hz	Time, s	Confining stress, kPa	σ'_1/σ'_3	G/G_{max}	D	γ_{ref}, %	m
Zhou *et al.* (2017)	HZY-1	300/750	SU	--	0.8	--	1000	1.5	yes	yes	0.0216	0.7293
							2000	1.5	yes	yes	0.0284	0.7346
							2000	2.5	yes	yes	0.0456	0.6430
							3000	1.5	yes	yes	0.0376	0.5973
							3000	2.5	no	yes	--	--
	HZY-2	300/750	SU	--	0.8	--	1000	1.5	yes	yes	0.0219	0.8883
							2000	1.5	yes	yes	0.0292	0.8234
							2000	2.5	yes	yes	0.0364	0.8247
							3000	1.5	yes	yes	0.0315	0.8346
							3000	2.5	no	yes	--	--
	HZY-3	300/750	SU	--	0.8	--	1000	1.5	yes	yes	0.0231	0.7658
							2000	1.5	yes	yes	0.0303	0.7269
							2000	2.5	yes	yes	0.0453	0.7790
							3000	1.5	yes	yes	0.0390	0.7532
							3000	2.5	no	yes	--	0.0000
	HZY-4	300/750	SU	--	0.8	--	1000	1.5	yes	no	0.0263	0.9000
							2000	1.5	yes	no	0.0242	0.8952
							2000	2.5	yes	no	0.0393	0.8385
							3000	1.5	yes	no	0.0400	0.7393
	LHK-1	300/750	SU	--	0.5	--	1500	2	yes	no	0.0278	0.9146
							500	2	yes	no	0.0198	0.7441
							3000	2	yes	no	0.0390	0.8188
Araei *et al.* (2012a)	S.G	300/600	DD	10	1	10	100	2	yes	yes	0.0386	0.9805
				5		5	100	2	yes	yes	0.0392	0.9821
				10		10	300	2	yes	yes	0.0394	0.9482
				5		5	300	2	yes	yes	0.0407	0.9439
				10		10	500	2	yes	yes	0.0430	1.5243
				5		5	500	2	yes	yes	0.0413	1.5035
				10		10	1000	1	yes	yes	0.0386	1.1513
				5		5	1000	1	yes	yes	0.0403	1.1503
			SU	10	1	10	100	2	yes	yes	0.0252	0.9935
				5		5	100	2	yes	yes	0.0264	0.9855
				10		10	300	2	yes	yes	0.0257	0.8707
				5		5	300	2	yes	yes	0.0276	0.8616
				10		10	500	2	yes	yes	0.0219	1.1758
				5		5	500	2	yes	yes	0.0217	1.1776
				10		10	1000	1	yes	yes	0.0292	1.1706
				5		5	1000	1	yes	yes	0.0316	1.1678
	S.3AMES	300/600	SU	10	0.1	100	200	1	yes	yes	0.0153	1.0881
				10	0.1	100	700	1	yes	yes	0.0211	0.9618
	S.3BMES	300/600	SU	10	0.1	100	200	1	yes	yes	0.0184	0.9143
				10	0.1	100	700	1	yes	yes	0.0343	0.7829
Araei *et al.* (2012b)	S.SBU	300/600	SU	40	0.1	400	100	1	yes	yes	0.0108	0.6878
					0.2	200	100		yes	yes	0.0098	0.6582
					0.5	80	100		yes	yes	0.0087	0.6187
					1	40	100		yes	yes	0.0088	0.6928
					2	20	100		yes	yes	0.0085	0.8296
					5	8	100		yes	yes	0.0053	0.7209
					10	4	100		yes	yes	0.0038	0.8476
			SU	40	0.1	400	200	1	yes	yes	0.0246	0.7206
					0.2	200	200		yes	yes	0.0225	0.6728
					0.5	80	200		yes	yes	0.0147	0.6060
					1	40	200		yes	yes	0.0119	0.6649
					2	20	200		yes	yes	0.0103	0.6039
					5	8	200		yes	yes	0.0077	0.8140
					10	4	200		yes	yes	0.0065	0.6520
			SU	40	0.1	400	400	1	no	yes	--	--
					0.2	200	400		no	yes	--	--
					0.5	80	400		yes	yes	0.0330	0.9206
					1	40	400		yes	yes	0.0311	0.7544
					2	20	400		yes	yes	0.0242	0.6905
					5	8	400		yes	yes	0.0184	0.6521
					10	4	400		yes	yes	0.0086	0.8573
			SU	40	0.1	400	600	1	yes	yes	0.0328	0.9250
					0.2	200	600		yes	yes	0.0356	0.8926
					0.5	80	600		yes	yes	0.0338	0.8305
					1	40	600		yes	yes	0.0257	0.6540
					2	20	600		yes	yes	0.0194	0.6300
					5	8	600		yes	yes	0.0111	0.8667
					10	4	600		yes	yes	0.0097	0.7639
			SU	40	0.1	400	1000	1	yes	yes	0.0668	0.5423
					0.2	200	1000		yes	yes	0.0280	0.7813
					0.5	80	1000		yes	yes	0.0452	0.6483
					1	40	1000		yes	yes	0.0421	0.5887
					2	20	1000		yes	yes	0.0384	0.5449
					5	8	1000		yes	yes	0.0230	0.5759
					10	4	1000		yes	yes	0.0128	0.8570
			SU	40	0.1	400	1500	1	yes	yes	0.0590	0.7262
					0.2	200	1500		yes	yes	0.0537	0.6421
					0.5	80	1500		yes	yes	0.0361	0.8468
					1	40	1500		yes	yes	0.0430	0.6611
					2	20	1500		yes	yes	0.0329	0.6837
					5	8	1500		yes	yes	0.0268	0.6519
					10	4	1500		yes	yes	0.0059	1.5480
Goto *et al.* (1992)	Depth 5-6 m	300/600	SU	10	0.01	1000	128	--	yes	yes	0.0463	0.9687
									yes	yes	0.0474	1.1530
	Depth 12-13 m						186		yes	yes	0.0802	1.3189
									yes	yes	0.0511	1.0699
Yasuda and Matsumoto (1994)	Angular	300/600	DD	12	0.2	60	100	--	yes	no	0.0256	1.0785
							200		yes	no	0.0267	1.0471
							300		yes	no	0.0337	0.9868
Hatanaka *et al*. (1988)	U-4	300/600	SU	3	0.01	300	294	--	yes	yes	0.0654	0.8339
									yes	yes	0.0632	0.8700
	U-5						491		yes	yes	0.0381	0.9813
									yes	yes	0.0524	1.1057

d, *h*: sample diameter and height, SU: saturated undrained, DD: dry drained, σ'_1, σ'_3: major and minor effective stress, γ_{ref}: reference shear strain, *m*: exponent

According to Ishihara (1996), the reference deformation γ_{ref} reflects the transition from linear elastic to non-elastic behaviour. When the soil behaves elastically, strains are concentrated in the contact between particles, with little or no rotation, while non-linear behaviour occurs when the relative movement between grains begins. The non-linearity is a function of the fines content, since for a soil subjected to cyclic loading with a high fines content, it would tend to initiate a lower reference deformation and lose its stability due to interlocking, causing a greater reduction in shear modulus *G*. However, in coarse soils, the loss of stability by interlocking requires a greater mobilizing strain, causing a lower reduction in *G* (Rollins *et al.*, 2020).

For this reason, it is necessary to quantify γ_{ref} as accurate as possible. In this context, there are different formulations to determine the value of γ_{ref} and *m*. Such is the case by Stokoe *et al.* (1999), who proposed an average value of m = 0.87 for sands, resulting relatively independent of the void ratio and confining stress. For gravels, Rollins *et al.* (1998) suggested average values of m = 0.84 and γ_{ref} = 0.04.

Based on the analysis performed by Stokoe *et al.* (1999) and data by Rollins *et al.* (1998), Rollins *et al.* (2020) propose for gravels an expression for γ_{ref} as a function of the confining stress, defined as:

$$\gamma_{\text{ref}} = a(\sigma_c')^b \tag{2}$$

where σ_c' is the confining stress in kPa, a = 0.0039 and b = 0.42. Since these values of a and b are relatively close to those proposed for sands (a = 0.0063, b = 0.38 (Darandeli, 2001; Rollins *et al.*, 2020)), although γ_{ref} is higher in sands than in gravels for the same value of σ_c', this difference is generally considered negligible (Kokusho *et al.*, 2005; Rollins *et al.*, 2020). So, combining (1) and (2) results:

$$\frac{G}{G_{\max}} = \frac{1}{1+\left(\frac{\gamma}{0.0039(\sigma_c')^{0.42}}\right)^{0.84}} \tag{3}$$

Then, expression (3) can provide for gravels curves of G/G_{max} as a function of the shear strain γ and the confining stress σ_c', which tend to be more linear as σ_c' increases and below the curves for sands (Darandeli, 2001). Additionally, Menq (2003) proposes an expression for γ_{ref} versus σ_c' which includes the influence of the uniformity coefficient C_u. Following this idea of including C_u, Rollins *et al.* (2020) derived another expression for $\gamma_{ref} = f(\sigma_c', C_u)$ based on statistical analyses of a much larger database.

$$\frac{G}{G_{\max}} = \frac{1}{1+\left(\frac{\gamma}{0.0046(C_u)^{-0.197}(\sigma_c')^{0.52}}\right)^{0.84}} \tag{4}$$

In expression (4), the gravel stiffness increases with σ_c' reducing the stiffness degradation. Conversely, when C_u increases, the curves of $G/G_{max} - \gamma$ move downwards and to the left because of the lower value of γ_{ref}.

Frequency and fines content effects

The dominant frequency in seismic events has been found to be below 15 Hz (Araei *et al.*, 2012a,b), although it may range between 0.01 Hz and 30 Hz (Meng, 2007). For that reason, a loading frequency range between 0.01 Hz and 10 Hz has been usually adopted in experimental studies as shown in Table 2. Taken the data from Table 2 and plotting G/G_{max} as a function of γ and γ_{ref}, where γ_{ref} is expressed as a function of σ_c' and the loading frequency *f*, results:

$$\gamma_{\text{ref}} = \frac{0.0033(\sigma_c')^{0.305}}{f^{0.242}} \tag{5}$$

$$\frac{G}{G_{\max}} = \frac{1}{1+\left(\frac{\gamma f^{0.242}}{0.0033(\sigma_c')^{0.305}}\right)^{0.858}} \tag{6}$$

In Figure 2, measured and estimated 946 values of G/G_{max} are compared, where the statistical analysis indicates that when using (6) approximately 85.6% of the data fall within the ± 25% error band, while only 2.2% is outside ± 50%. Whereas, measured and estimated 922 values of G/G_{max} using (4) results in 60.5% of the data falling within ± 25%, and 16.8% are outside ± 50% of error. Therefore, the use of (5) and (6) can lead to an enhancement in the prediction of G/G_{max}. Moreover, it can be observed that data from expression (6) is distributed symmetrically around the 1:1 centre line, which is in contrast with the data from expression (4) leaning on the left side of the plot resulting in many outlier points.

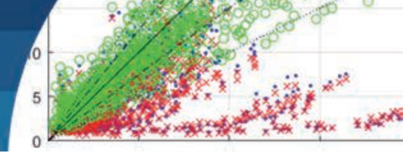

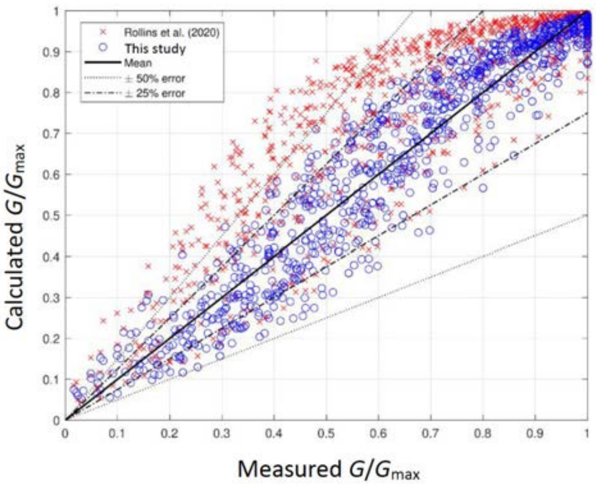

Figure 2: Comparison between measured and estimated G/G_{max} using Rollins *et al*. (2020) formulation (4) and this study proposal using expressions (5) and (6)

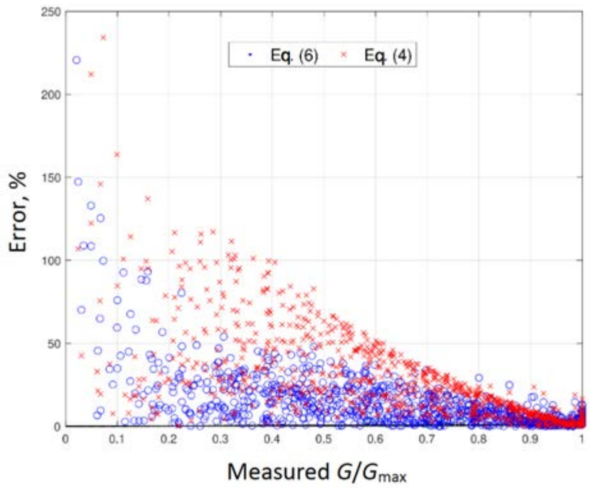

Figure 3: Error in estimating G/G_{max} comparing Rollins *et al*. (2020) formulation (4) and this study proposal (6)

Figure 3 shows the error in estimating G/G_{max}. It can be observed that for $G/G_{max} = 0.5$, *i.e.* γ_{ref}, the error is concentrated under 50% for the data calculated using expression (6), whereas the points calculated with expression (4) can reach approximately 75% error. For values close to 85% of G/G_{max}, the error decreases almost similarly for both formulations.

Figure 4 shows the data points from the cyclic triaxial tests presented in Table 2. It is clear to see the scatter in the progressive degradation of stiffness with the shear strain between 0.1% and 0.001%. Due to this scatter, the need arises to be able to recalibrate a single characteristic curve whose purpose is to improve the representation of the G/G_{max} variation. In this context, the mean variation

a)

b)

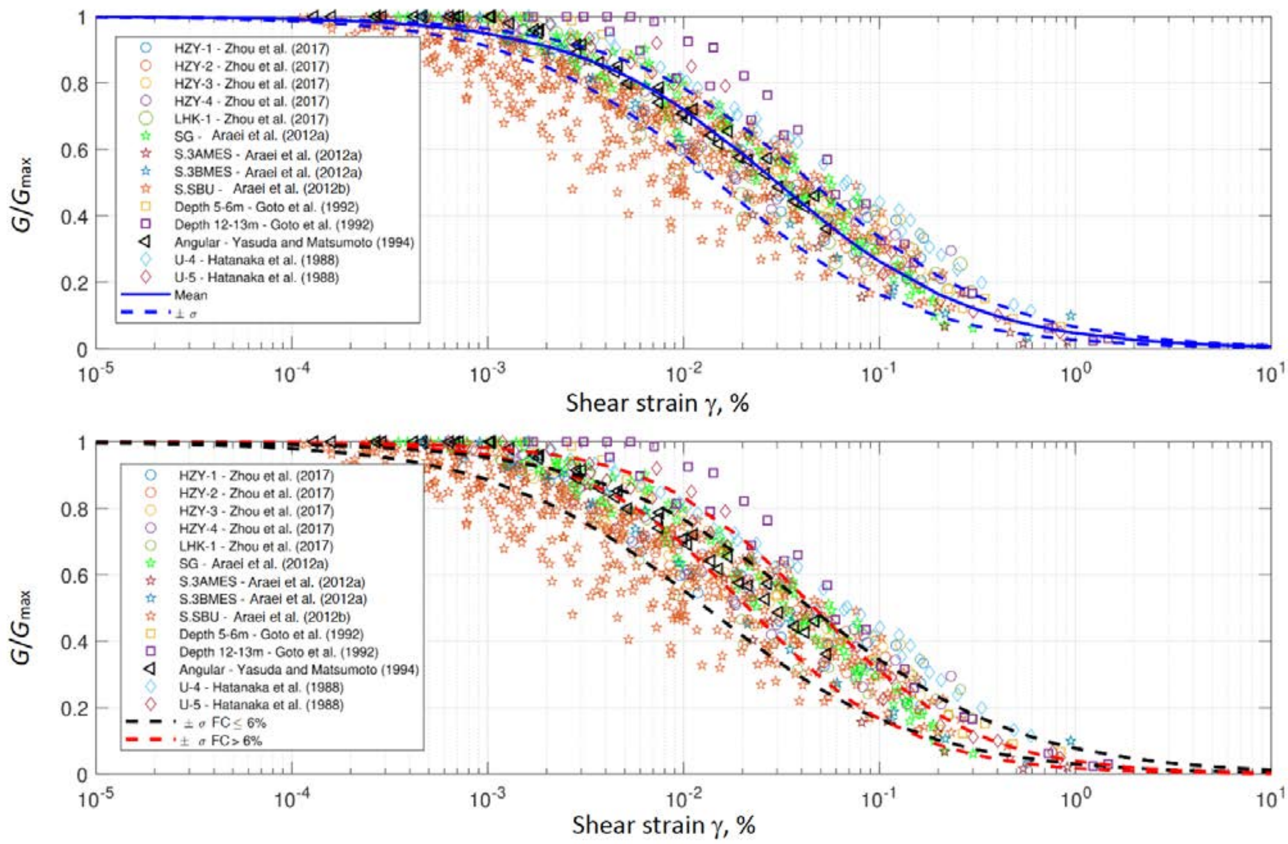

Figure 4: Variation of G/G_{max} versus γ including measured data points (Tabla 2) and curves of best fit with a) limits of ± one standard deviation σ and b) limits of ± σ for the classification by fines content FC

(continuous line) with its respective ± standard deviation Sd (segmented lines) is plotted using expression (1). Therefore, according to the statistical analysis, the average values are; $\gamma_{ref} = 0.030 \pm Sd_\gamma = 0.015$ and $m = 0.858 \pm Sd_m = 0.212$.

In order to be able to better differentiate the gravel dynamic response in terms of shear stiffness, the data was divided in two groups according to the sample fines content FC. This division was established at FC = 6%, as shown in Figures 4b, 5a and 5b. For a level of shear stress of less than 0.1%, the best fitted curves to the data with FC > 6% are slightly to the right side and with steeper slope, *i.e.* higher stiffness variation than for the data with FC ≤ 6%. However, for shear strains greater than 0.1%, the opposite tends to occur. The best fit of the data corresponds to the regression analysis that combines both groups, since the errors in the estimation individually were slightly greater than the data set treated as only one group. From the regression analyses, the parameter values that best fit the data for FC ≤ 6% are: $\gamma_{ref} = 0.029 \pm Sd_{\gamma ref} = 0.016$ and $m = 0.797 \pm Sd_m = 0.179$, whilst for FC > 6%: $\gamma_{ref} = 0.034 \pm Sd_{\gamma ref} = 0.013$ and $m = 1.047 \pm Sd_m = 0.190$.

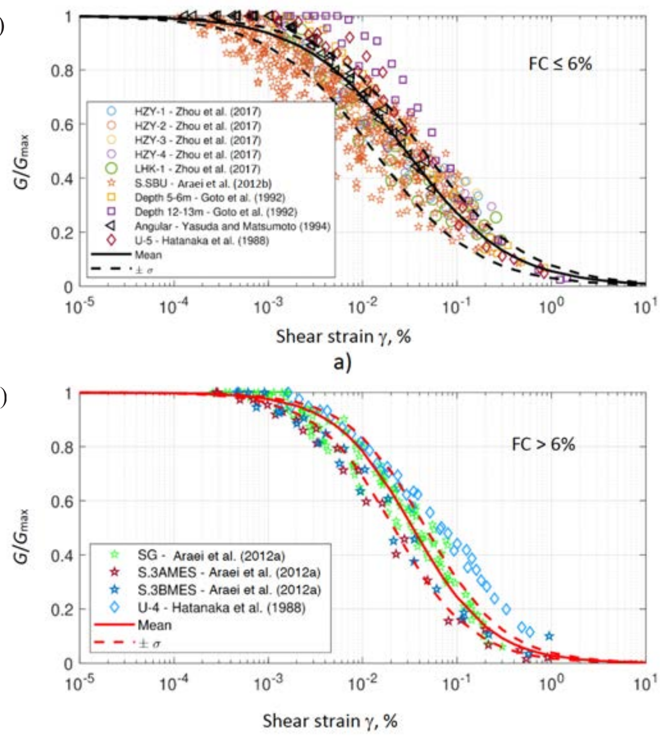

Figure 5: Data division respect to the fines content FC: a) ≤ 6% and b) > 6%

Figure 6 shows a three dimensional plot with the database from Table 2 including the formulation proposed in (5) and (6) in terms of G/G_{max} as a function of γ and f. It can be observed that most of the data is for low values of loading frequency and the stiffness degradation pattern tends to be similar for the entire frequency range analysed. Therefore, loading frequency does not really influence significantly the shear modulus G at least for the frequency range considered in these analyses. This is not in agreement with Araei *et al.* (2012a), who conclude for their data that the increase in loading frequency f does increase G, but at low strain, because as strain increases the G increase rate reduces with the increase of f. Moreover, Araei *et al.* (2012a) also conclude that $G/G_{max} - \gamma$ decreases when f increases for a certain value of strain. More data is then needed for higher values of frequency (f > 10 Hz) to validate the applicability of the proposed formulation.

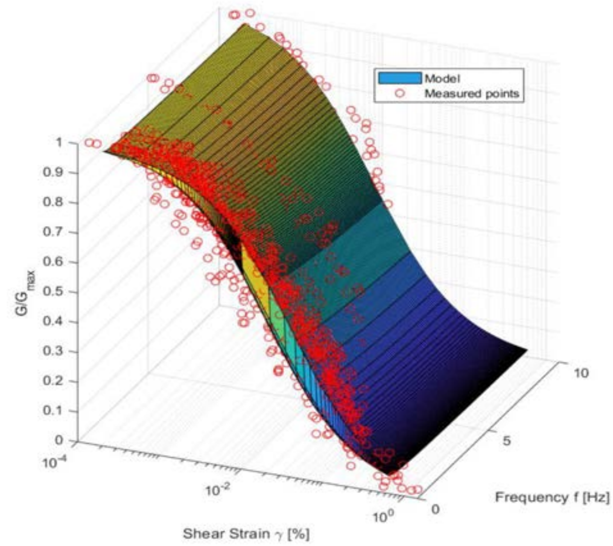

Figure 6: 3D plot for $G/G_{max} = f(\gamma, f)$ data and formulation proposed

Damping ratio *D*

Damping is a definition for the dissipation of stored energy during cyclic loading. Damping ratio D is the normalisation of the dissipated energy by the stored elastic strain energy. For sands, it has been known that D is small and constant for very low levels of cyclic shear strains γ (< 10^{-4} %), however, it can increase steadily with higher values of γ (*e.g.* Hardin, 1965; Hardin and Drnevich, 1972a,b; Martínez, 2008; Navarrete, 2009). Therefore, under strong cyclic loading D can vary and the use of only one low or medium D value is an oversimplification that may not always allow adequate dynamic analyses. The study of D for gravels started in the middle of the 1980s and a summary of available results has been reported by Rollins *et al.* (1998, 2020). From the database available, Rollins *et al.* (1998) proposed the following best fit hyperbolic expression for D:

$$D = 0.8 + 18(1 + 0.15\gamma^{-0.9})^{-0.75} \quad (7)$$

where D and γ are in percentage. It has been found that the use of (7) generally can over or underestimate D in around 25% for $D > 10\%$, whereas for $D < 10\%$, the variation of D can be of 50% or even more. Another approach was followed by Stokoe *et al.* (1999) when they proposed that D could be estimated by means of G/G_{max} using a modified version of the Masing rule and the number of cycles. However, it has been argued that the Masing approach overestimates D in particular at high strain levels (*e.g.* Hardin and Drnevich, 1972a; Vucetic and Dobry, 1991). Moreover, the Masing rule approach results in $D = 0$ in the small strain range (Darandeli, 2001). Despite these observations, Rollins *et al.* (2020) present a modified Masing formulation considering $D_{min} = 1\%$, typical value from the database analysed. Confining stress σ'_c and uniformity coefficient C_u are implicitly introduced through G/G_{max} formulations, resulting in D-γ curves bounded by (7) with $D \pm 30\%$, showing that D tends to decrease with σ'_c and increase with C_u. This confirms that damping has an opposite behaviour compared to the shear modulus. However, the Masing approach leads to similar over and underestimations as those obtained by (7).

In order to obtain an explicit relationship for $D = f(\sigma'_c, C_u)$, *i.e.* without G/G_{max}, Rollins *et al.* (2020) developed the following expression from a regression analysis.

$$D = 26.05\left(\frac{\gamma}{1+\gamma}\right)^{0.375} C_u^{0.08}\sigma_c'^{-0.07} \quad (8)$$

Nevertheless, in statistical terms (8) is neither significantly better than (7) nor the Masing approach (Rollins *et al.*, 2020).

Frequency and fines content effects

In the same form as it was included in the stiffness analyses, frequency and fines content FC may affect the dynamic response of gravels. Taken the data from Table 2 and carrying out a best fit analysis, results in the following expressions:

$$D = \begin{cases} m\left(\frac{\gamma}{1+\gamma}\right)^{0.306} & , \text{FC} \le 6\% \\ m\left(\frac{\gamma}{1+\gamma}\right)^{0.236} & , \text{FC} > 6\% \end{cases} \quad (9)$$

$$m = 11.343f - 10.008\log(\sigma_c') + 45.331 \quad (10)$$

Figure 7 shows the plot with measured points and proposed curves by Rollins *et al.* (1998) and using (10). The scatter points away from the main trend represent the frequency effect (Araei *et al.*, 2012b). The proposed formulation aims to include the frequency effect in the estimation of D.

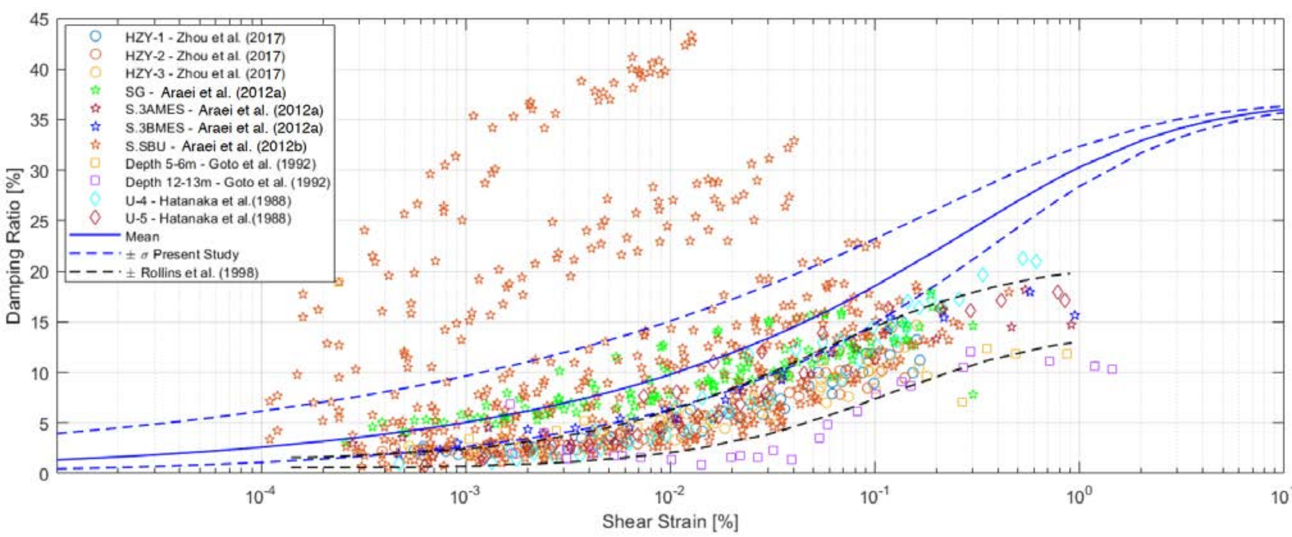

Figure 7: D- γ data and curves proposed by Rollins *et al.* (1998) and this study showing mean and standard deviation

Figure 8 shows the error between measured and estimated values of D, where for expression (7) by Rollins *et al.* (1998) and expression (8) by Rollins *et al.* (2020) the error is around 30% with the data points falling within the bands of 25% error from the 1:1 line of perfect measured-estimated agreement. By comparison, using (9) and (10) results in 56% of the data falling in the 25% error.

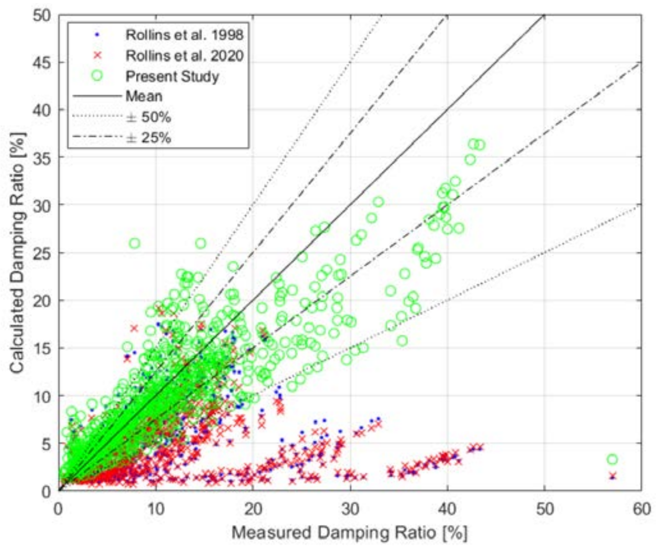

Figure 8: Comparison of D measured data with estimations from formulations by Rollins *et al*. (1998, 2020) and proposed in this study

The mean curve and standard deviation for (9) and (10) are strongly influenced by the data from Araei *et al.* (2012b), which is not included in the database of Rollins *et al.* (1998, 2020) and for that reason this curve is above the curve proposed by Rollins et al. (1998), as also shown in Figure 7.

Figure 9a shows results of D-γ for the fines content FC $\leq$ 6% where it can be observed significant scatter in the data and the curves from (9) and (10) predict higher D than those by Rollins *et al.* (1998). In Figure 9b for FC > 6%, there is less data and scatter and the same higher D is also predicted, although with some overlapping.

At higher levels of non-plastic fine material, it has been consistently reported in sands lower levels of damping ratio D and higher levels of shear modulus G (Navarrete, 2009; Wichtmann *et al.*, 2015). In gravels, Figure 10 shows similar trend for D in a 3D plot of D-γ-f where the curve from expression (9) for FC < 6% lies above the curve for FC $\geq$ 6%. Although, for low shear strain γ and low frequency f, both curves tend to converge underestimating measured D, when γ and f increase both curves steadily separate increasing D.

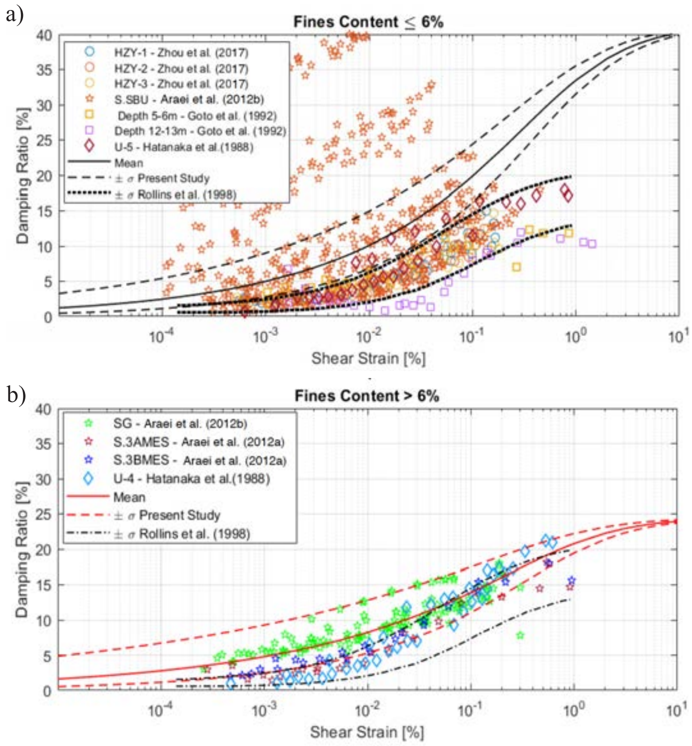

Figure 9: D- γ data and curves proposed by Rollins *et al.* (1998) and this study showing mean and standard deviation for: a) FC $\leq$ 6% and b) FC > 6 %

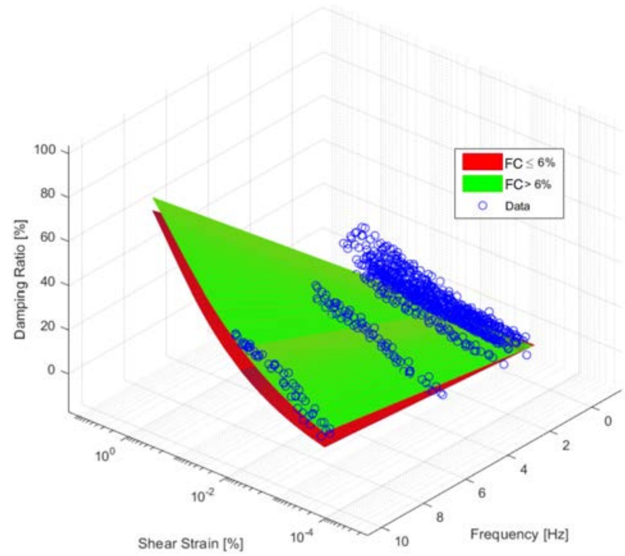

Figure 10: 3D plot for the data and formulations proposed for damping ratio D as a function of γ, f and FC

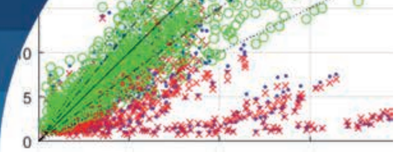

Conclusions

This study presents the analysis of a selected database of cyclic triaxial tests in gravely soils applying hyperbolic formulations for the variation of shear modulus and damping ratio as a function of shear strain. It has been confirmed that the confining stress affects the dynamic response of gravels as it has been previously reported (Rollins *at al.*, 2020). It has been found in this work that including the confining stress and the fines content a better estimation of G/G_{max} can be achieved, resulting in 85.6% of the data (in measured and estimated G/G_{max} plot) within an error band of ± 25%, which improve around 25% the previous formulation proposed by Rollins *et al.* (2020). In a plot of error versus estimated G/G_{max}, the error increases when $G/G_{max} \rightarrow 0$, *i.e.* large shear strains, however, the formulation proposed in this work can reduce this error up to 50% compared with that proposed by Rollins *et al*. (2020). Nonetheless, the error reduces and becomes similar for both approaches when $G/G_{max} \geq 0.8$ (small shear strains). The effect of the loading frequency is not significant on the estimation of G/G_{max}, which does not agree with some effect on the shear modulus found by Araei *et al.* (2012b). In contrast, the loading frequency does affect the damping ratio D as postulated by Araei *et al.* (2012b). From regression analyses and separating at 6% fines content, in a measured and estimated data plot of D resulted in 56% of the data points within a ± 25% band error. Further research is needed to increase the gravel data base for the analysis of extended ranges of loading frequency and fines content.

References

Araei, A.A., Tabatabaei, S.H. and Razeghi, H.R. (2012a). Cyclic and post-cyclic monotonic behavior of crushed conglomerate rockfill material under dry and saturated conditions. *Scientia Iranica* **19**(1), 64-76

Araei, A.A., Razeghi, H.R., Tabatabaei, S.H. and Ghalandarzadeh, A. (2012b). Loading frequency effect on stiffness, damping and cyclic strength of modeled rockfill materials. *Soil Dynamics and Earthquake Engineering* **33**(1): 1–18

ASTM D2487 (2017). Standard practice for classification of soils for engineering purposes (Unified Soil Classification System). West Conshohocken, PA, USA

Darendeli, M.B. (2001). *Development of a new family of normalized modulus reduction and material damping curves*. University of Texas at Austin, USA

Dorador, L. and Villalobos, F.A. (2020a). Scalping techniques in geomechanical characterization of coarse granular materials. *Obras y Proyectos* **28**, 24-34

Dorador, L. and Villalobos, F.A. (2020b). Analysis of the geomechanical characterization of coarse granular materials using the parallel gradation method. *Obras y Proyectos* **27**, 50-63

Goto, S., Suzuki, Y., Nishio, S. and Oh-Oka, H. (1992). Mechanical properties of undisturbed Tone River gravel obtained by in-situ freezing method. *Soils & Foundations* **32**(3), 15–25

Hardin, B.O. and Drnevich, V.P. (1972a). Shear modulus and damping in soils: design equations and curves. *Journal of the Soil Mechanics and Foundation Division* **98**(7), 667-692

Hardin, B.O. and Drnevich, V.P. (1972b). Shear modulus and damping in soils: measurement and parameter effects (Terzaghi lecture). *Journal of the Soil Mechanics and Foundation Division* **98**(6):603–624

Hardin, B.O. (1965). The nature of damping in sands. *Journal of the Soil Mechanics and Foundation Division* **91**(1), 63-67

Hatanaka, M., Suzuki, Y., Kawasaki, T. and Endo, M. (1988). Cyclic undrained shear properties of high quality undisturbed Tokyo Gravel. *Soils & Foundations* **28**(4), 57–68

Ishihara, K. (1996). *Soil behaviour in earthquake geotechnics.* Oxford University Press, UK

Kokusho, T., Aoyagi, T. and Wakunami, A. (2005). In-situ soil specific nonlinear properties back-calculated from vertical array records during 1995 Kobe Earthquake. *Journal of Geotechnical and Geoenvironmental Engineering* **131**(12): 1509–1521

Kramer, S.L. (1996). *Geotechnical earthquake engineering*. Pearson, USA

Martínez, R.A. (2008). Influencia de la granulometría en las propiedades dinámicas de suelos no cohesivos bajo pequeñas deformaciones. *Obras y Proyectos* **3**, 22-31

Meng, J. (2007). Earthquake ground motion simulation with frequency-dependent soil properties. *Soil Dynamics and Earthquake Engineering* **27**: 234–241

Menq, F.Y. (2003). *Dynamic properties of sandy and gravelly soils*. PhD thesis, University of Texas at Austin, USA

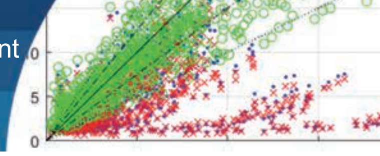

Navarrete, M. (2009). Influencia del contenido de finos no plástico en la rigidez y el amortiguamiento a bajas amplitudes de deformación en arenas cuarzosas. *Obras y Proyectos* **6**, 19-30

Ovalle, C., Linero, S., Dano, C., Bard, E., Hicher, P. Y. and Osses, R. (2020). Data compilation from large drained compression triaxial tests on coarse crushable rockfill materials. *Journal of Geotechnical and Geoenvironmental Engineering* **146**(9), 06020013

Rollins, K.M., Singh, M. and Roy, J. (2020). Simplified equations for shear-modulus degradation and damping of gravels. *Journal of Geotechnical and Geoenvironmental Engineering* **146**(9):04020076.

Rollins, K.M., Evans, M.D., Diehl, N.B., and Daily, W.D. (1998). Shear modulus and damping relationships for gravels. *Journal of Geotechnical and Geoenvironmental Engineering* **124**(5): 396–405

Stokoe, K.H., Darendeli, M.B., Andrus, R.D and Brown, L.T. (1999). Dynamic soil properties: laboratory, field and correlation studies. *2nd International Conference on Earthquake Geotechnical Engineering*, Lisboa, Portugal, Seco e Pinto, P.S. (ed.), Balkema, the Netherlands, 811–845

Vucetic, M. and Dobry, R. (1991). Effect of soil plasticity on cyclic response. *Journal of Geotechnical Engineering* **117**(1): 89–107

Wichtmann, T., Navarrete, M.A. and Triantafyllidis, T. (2015). On the influence of a non-cohesive fines content on small strain stiffness, modulus degradation and damping of quartz sand. *Soil Dynamics and Earthquake Engineering* **69**, 103-114

Yasuda, N. and Matsumoto, N. (1994). Comparisons of deformation characteristics of rockfill materials using monotonic and cyclic loading laboratory tests and in-situ tests. *Canadian Geotechnical Journal* **31**(2), 162–174

Zhou, W., Chen, Y., Ma, G., Yang, L. and Chang, X. (2017). A modified dynamic shear modulus model for rockfill materials under a wide range of shear strain amplitudes. *Soil Dynamics and Earthquake Engineering* **92**, 229-238